Electronic Supplementary Material (ESI) for Materials Chemistry Frontiers.

Supporting information

Crystalline porphyrin-based graphdiyne for electrochemical hydrogen and oxygen evolution reactions

Qingyan Pan, [a+] Xinsheng Chen, [a+] Hui Liu, [a] Weijin Gan, [a] Naixiu Ding,*[a] and Yingjie Zhao*[a]

Engineering Research Center of High Performance Polymer and Molding Technology, Ministry of Education, College of Polymer Science and Engineering, Qingdao University of Science and Technology, Qingdao 266042, China

[*] Corresponding Authors: nxding1717@163.com; yz@qust.edu.cn

[+] These authors contributed equally to this work.

Table of Contents

1. Supporting Methods

2. Supporting Figures

1. Supporting Methods

1.1. Materials and Methods

All reactions were carried out under Argon condition unless otherwise noted. Tetrabutyamonium fluride (TBAF, 1.0 M solution in THF) was obtained from TCI (China) and used without further purification. 3-(trimethylsilyl)propiolaldehyde, pyrrole, DDQ, and Boron trifluoride diethyl etherate were purchased from Energy Co.Ltd. Unless otherwise specified, all other reagents were purchased commercially from Tansole and used without further purification. All aqueous solutions were prepared with Milli-Q water.

^{1}H-NMR spectra were performed on 400 MHz spectrometers (Bruker AVANCE NEO 400 Ascend) in the indicated solvents at room temperature. MALDI-TOF mass spectrometry analysis was performed on a Bruker Microflex-LRF mass spectrometer in positive ion. SEM images were collected using a scanning electron microscope (JEOL, JSM-7500F) at an accelerating voltage of 5.0 kV. TEM was performed on a JEM-2100 electron microscope with an accelerating voltage of 200 kV. The ultraviolet, visible and near-infrared absorbance was measured by an Ultraviolet visible near-infrared spectrophotometer (Agilent, cary5000). XPS was performed on a Thermo Scientific ESCALab 250Xi instrument. The parameters were as follows: Al Kα (1486.6 eV, 150 W) radiation was used as the X-ray source, the vacuum degree of the chamber was 3.6×10^{-9} mbar and the scan range was -10~1350 eV. The spectra were analyzed using Avantage Software. Raman spectrum was investigated on HORIBA Raman spectrometer (LabRAM HR Evolution), with an excitation wavelength at 532 nm and spot diameter for 1 μm. A typical three-electrode system (CHI 760E, CH Instruments, Inc. Shanghai) was used for all electrochemical measurements.

Electrochemistry:

Electrochemical experiments were conducted at a CHI760E electrochemical workstation of Shanghai Chenhua instrument using a traditional three-electrode battery system. In all electrochemical tests, the platinum sheet (1×1 cm^2) electrode was used for the counter electrode. To prepare the working electrode, catalyst (2 mg) and Nafion solution (DuPont 5 wt%, 40 μL) were dispersed in a 300 μL mixture solution consisting of deionized water (150 μL) and EtOH (150 μL). Obtained uniform catalyst solution (50 μL) was decorated onto a 1 × 1 cm carbon cloth (**CC**) and dried at room temperature affording the desired working electrode (loading content: 0.28 mg/cm^2).

In the hydrogen evolution reaction (HER) test, the catalyst-modified **CC**, mercury/mercury oxide electrode (Hg/HgO, MOE) and 1.0 M KOH solution were used as the working electrode, reference electrode and electrolyte, respectively. The conversion of potential based on the following equation, $E_{RHE} = E_{Hg/HgO} + 0.0592\ pH + 0.098$. In the measurement of oxygen evolution reaction (OER), the Hg/HgO-MOE and 1.0 M KOH solution were used as the reference electrode and electrolyte, respectively. The working electrode was the same as the test of HER. The conversion of potential according to the following equation, $E_{RHE} = E_{Hg/HgO} + 0.0592\ pH + 0.098$. All linear sweep voltammetry (LSV) measurements were recorded at a scan rate of 5 mV/s. The long-term stability of HER and OER is achieved through the chronoamperometry experiment. To estimate the electrochemical surface area (ECSA) of the prepared catalyst, the electrochemical double-layer capacitance (Cdl) was determined based on the double-layer charging curves using CVs records at different scanning speeds of 20, 40, 60, 80 and 100 mV/s. The electrochemical impedance spectroscopy (EIS) was performed with a frequency range of 10^{-1} to 10^{5} Hz.

1.2 Synthesis

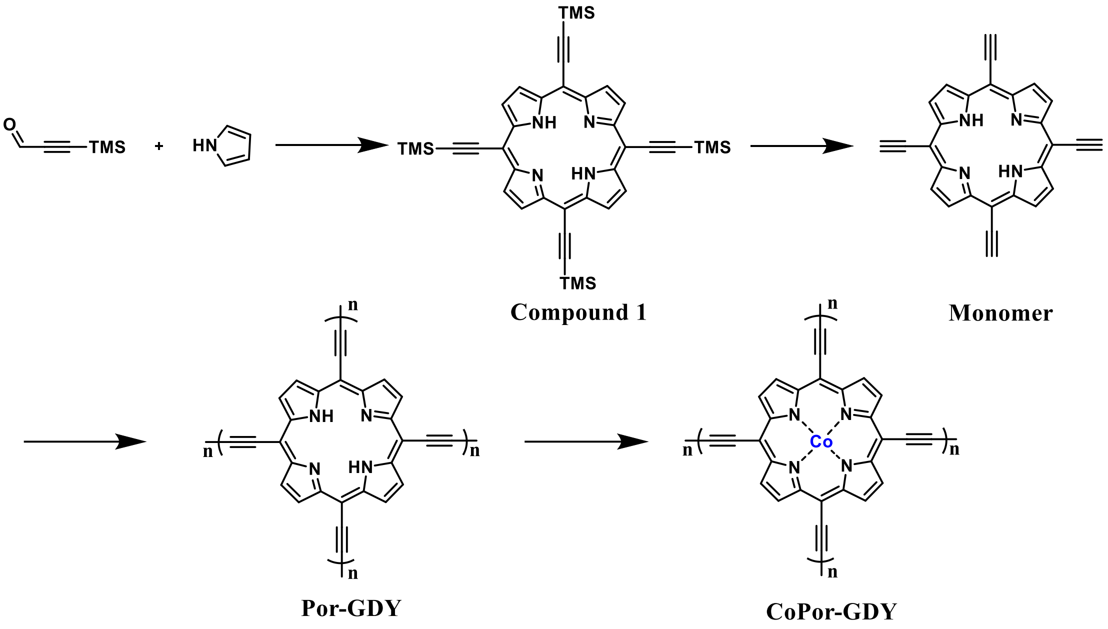

Scheme S1. Synthetic of **Por-GDY** and **CoPor-GDY**

Compound 1.[1] A mixture of dichloromethane (300 mL), 3-(trimethylsilyl) propiolaldehyde (370 µL, 2.5 mmol) and pyrrole (175 µL, 2.5 mmol) was stirred in a 500 mL flask at -40 °C. Boron trifluoride ether (40 µL, 325 µmol) was added and then the temperature was naturally increased to 25 °C. After further stirring for 8 h, DDQ

(570 mg, 2.5 mmol) was added. After 3 h, the reaction solution was concentrated and purified by silica gel column chromatography (eluent: ethyl acetate/petroleum ether = 1/5 v/v). The crude product was recrystallized from a mixed solvent of methanol and dichloromethane to give 40 mg of product (yield: 9.2%). ^{1}HNMR ($CDCl_3$,400 MHz): 9.47(s, 8H), 0.65(s, 36H), -2.16(s, 2H);

Por-GDY. To a solution of compound **1** (62 mg, 0.09 mmol) in 100 mLTHF was added TBAF (0.72 mL of 1 M THF solution) and stirred at 0 °Cfor 10 min. The solution was then diluted with ethyl acetate and washed with brine and dried with anhydrous Na_2SO_4. The solvent was removed in vacuo and the obtainedmonomerwasused directly without further purification. The monomer wasdissolved with 80 mL pyridine and added slowly over 8 h to a solution of copper foils in 100 mL pyridine at 80 °C. In this process, the Cu foil wasused not only as a catalyst source but also as a template for the growth of 2D **Por-GDY**. In the presence of pyridine, trace amounts of Cu(II) ions can be generated on the surface of the Cu foil. The induction time is strongly dependent on the concentration of monomer or catalyst during the polymerization. In the beginning, the concentration of Cu(II) ions and monomer are very diluted, so the heterogeneous nucleation and polymerization occurred preferentially on the surface of Cu foil. The nucleation can be controlled to arise primarily on the surface of Cu foil resulting in the formation of many active nucleation centers, which minimize the interfacial energy barrier and lead to subsequently the growth of **Por-GDY** on the surface of Cu foil. Besides, the templating effect of the catalytically active 2D surface leads to the formation of thermodynamically stable, conjugated 2D **Por-GDY**. With the increase of monomer, the concentrated monomer leads to homogeneous nucleation and faster polymerization in solution than that of on Cu foil substrate. So **Por-GDY** nanoparticles can also be observed as precipitation, which could suppress the growth rate of **Por-GDY** on the Cu foil. After 3days reaction at 80 °C in dark, the copper foils were washed with acetone and DMF in turn and a black film was obtained on the copper foil.

CoPor-GDY. The synthesized **Por-GDY** (20 mg), $CoCl_2$ (80 mg) and DMF (10 mL) were placed in a flask. The obtained mixture was uniformly dispersed by ultrasonic treatment, followed by heating at 120 ℃ for 24 h. After the reaction was completed, the precipitate was obtained via filtration and washed with deionized water and EtOH. The product was dried under vacuum for 12 h to obtain the desired **CoPor-GDY** material as a gray dark powder (16 mg).

1.3 AB Stacking mode analysis for Por-GDY and CoPor-GDY

Table S1. Fractional atomic coordinates for the unit cell of **Por-GDY** and **CoPor-GDY** with AB stacking.

Symmetry Group	FMMM(D2H-23)						
a = 19.4498, b = 19.5420, c = 6.2966, α = β = γ = 90°							
C1	0.5581	0.1506	0.0000	**C7**	0.7243	0.7754	0.0000
C2	0.5355	0.2180	0.0000	**H8**	0.5674	0.2634	0.0000
C3	0.6277	0.1292	0.0000	**H9**	0.2348	0.0673	0.0000
C4	0.3496	0.0589	0.0000	**N10**	0.5000	0.1063	0.0000
C5	0.2806	0.0355	0.0000	**N11**	0.3950	0.0000	0.0000
C6	0.3197	0.8187	0.0000	**H12**	0.4474	0.0000	0.0000

1.4 References

1. Anderson, H. L. Meso-alkynyl porphyrins. *Tetrahedron Lett.* **1992**, *33*, 1101-1104.

2. Supporting Figures

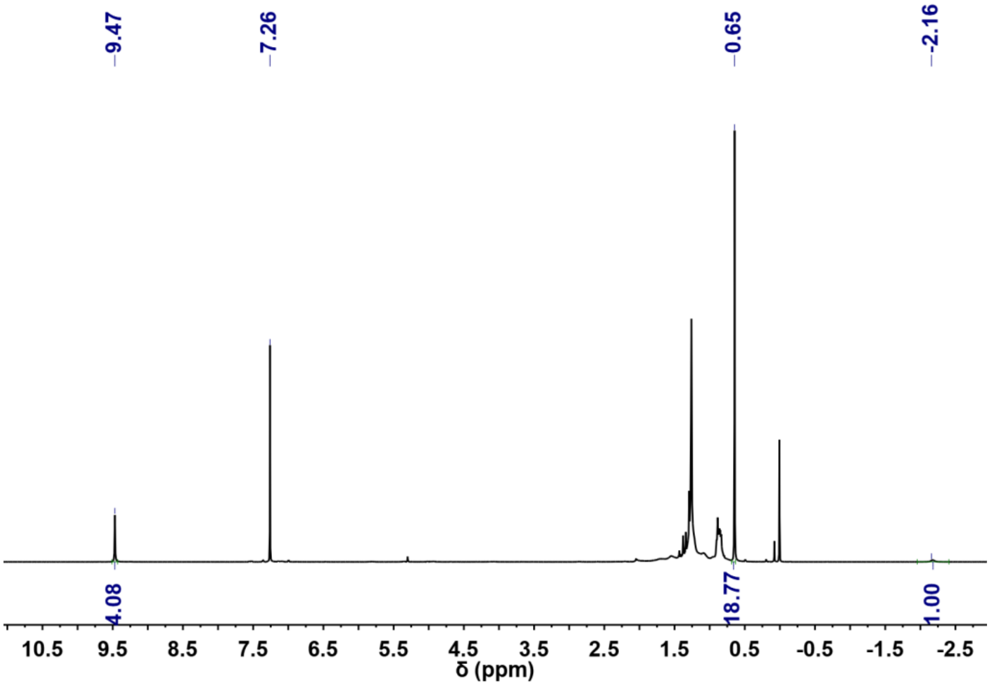

Figure S1. ^{1}H NMR of compound **1** in $CDCl_3$ at 25 ℃.

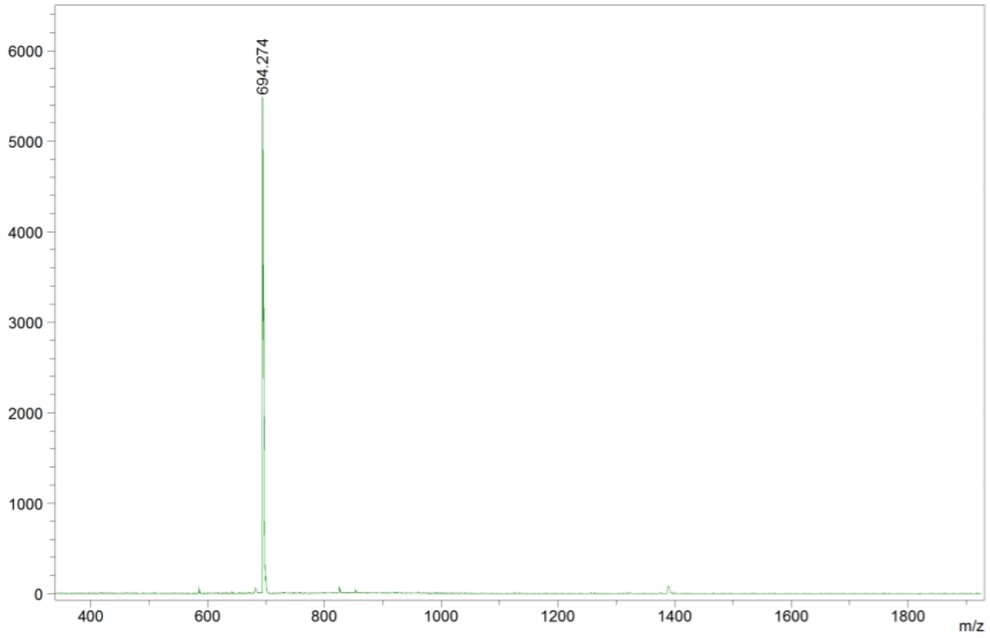

Figure S2. MALDI-TOF result of compound **1**.

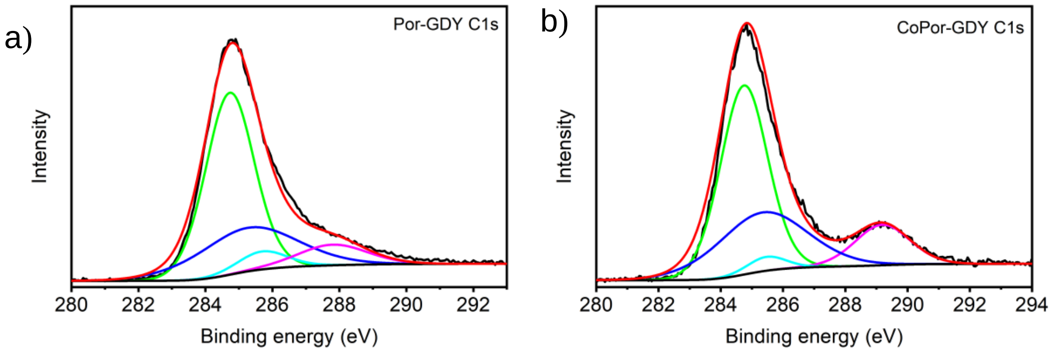

Figure S3. High-resolution asymmetric C1s XPS spectrum of a) **Por-GDY** and b) **CoPor-GDY**.

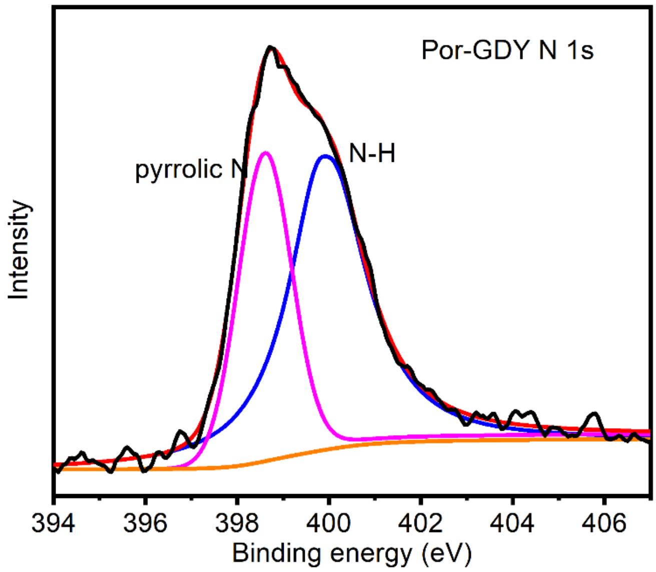

Figure S4. High-resolution asymmetric N1s XPS spectrum of **Por-GDY**.

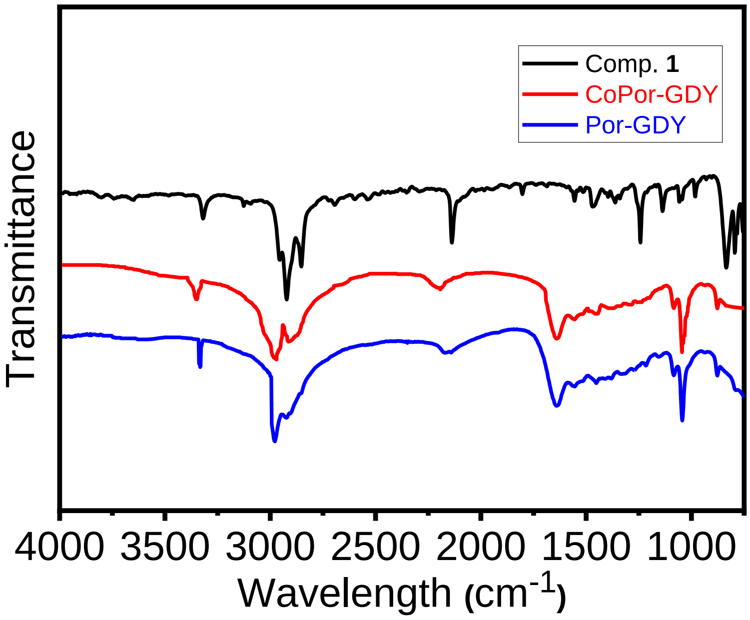

Figure S5. FTIR spectra of compound **1**, **Por-GDY** and **CoPor-GDY**.

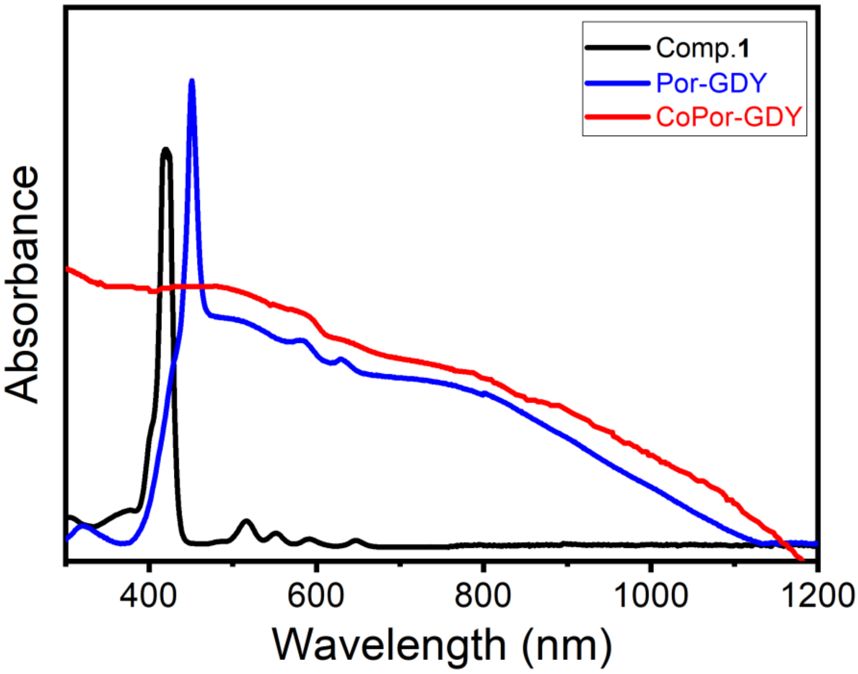

Figure S6. UV-vis spectrum of compound **1**, **Por-GDY** and **CoPor-GDY**.

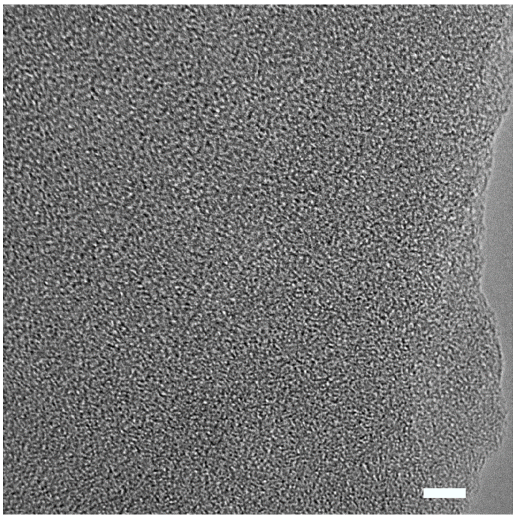

Figure S7. High-resolution TEM image of **CoPor-GDY**. (bar 5 nm)

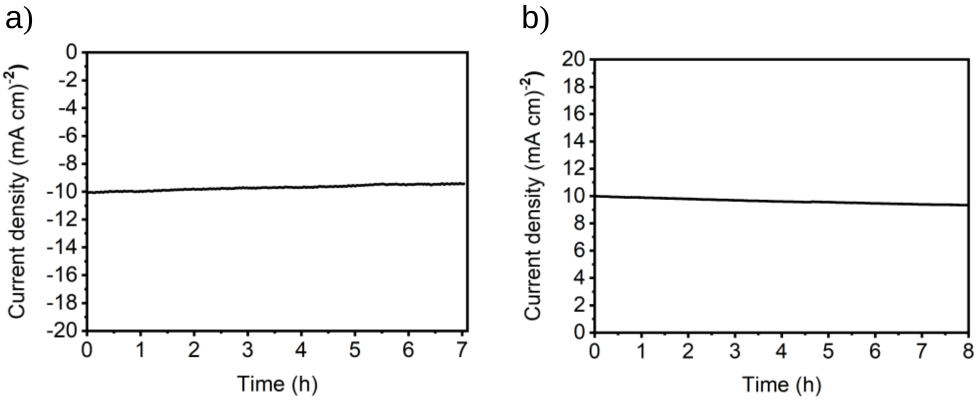

Figure S8. Time-dependent stability of **CoPor-GDY** for a) HER and b) OER.

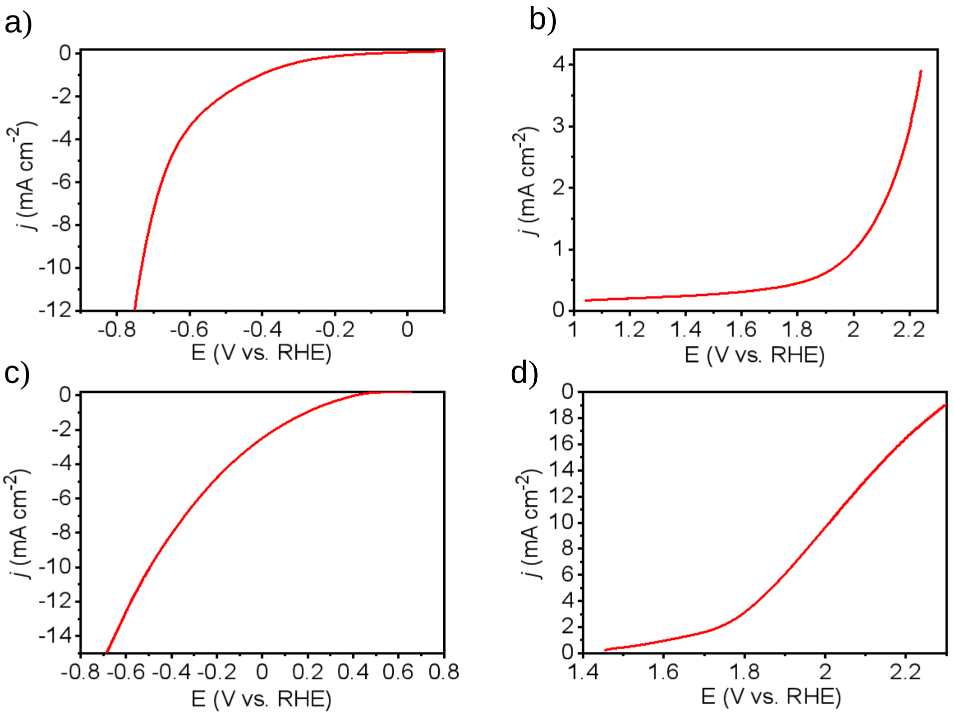

Figure S9. The electrocatalytic performances of **CoPor-GDY** in acidic and neutral solution. a) HER LSV curve in 0.5 M H_2SO_4, with an overpotential is 730 mV and a Tafel slope of 246 mV dec^{-1}; b) OER LSV curve in 0.5 M H_2SO_4, with an overpotential is more than 1000 mV and a Tafel slope of 196 mV dec^{-1} for OER.c) HER LSV curve in 0.2 M PBS, with an overpotential is 500 mV and a Tafel slope of 1016 mV dec^{-1}; d) OER LSV curve in 0.2 M PBS, with an overpotential is 700 mV and a Tafel slope of 616 mV dec^{-1}.

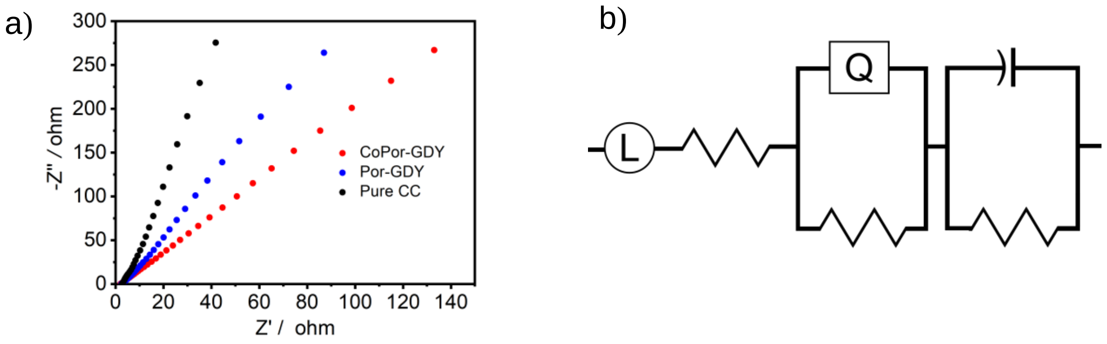

Figure S10. a) EIS Nyquist plots of the catalysts. b) The circuit equivalent model of used for the data fitting.

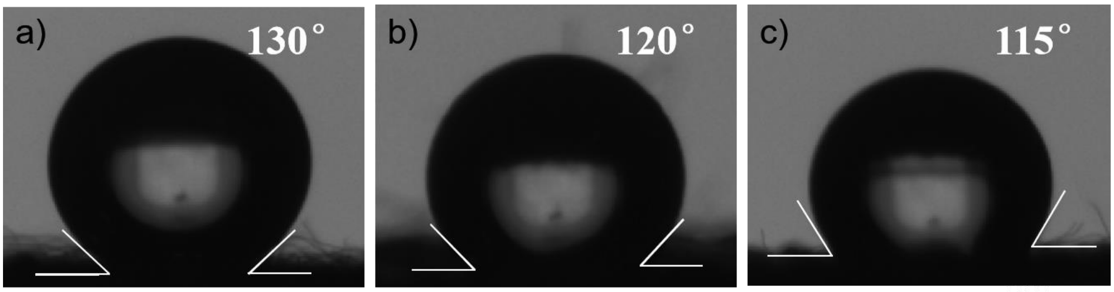

Figure S11. Contact angle measurements of three electrodes: a) pure **CC**, b) **Por-GDY@CC** and c) **CoPor-GDY@CC**.

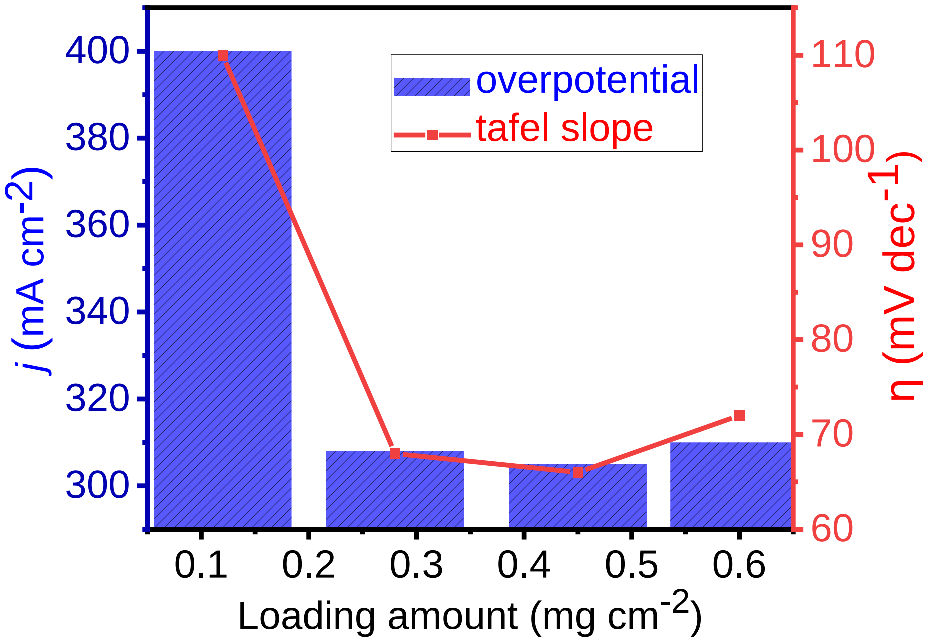

Figure S12. HER performances of **CoPor-GDY** at different loading amounts.